TRANSMISSION PROPERTIES OF TWO SHIFTED MAGNETOINDUCTIVE WAVEGUIDES

A. Radkovskaya,[1] O. Sydoruk,[2] M. Shamonin,[3] C. J. Stevens,[4] G. Faulkner,[4] D. J. Edwards,[4] E. Shamonina,[4] and L. Solymar[5]
[1] Magnetism Division, Faculty of Physics, M. V. Lomonosov Moscow State University, Leninskie Gory, Moscow 119992, Russia
[2] Department of Physics, University of Osnabrück, Osnabrück D-49069, Germany
[3] Department of Electrical Engineering and Information Technology, University of Applied Sciences, Regensburg D-93025, Germany
[4] Department of Engineering Science, University of Oxford, Parks Road, Oxford OX1 3PJ, United Kingdom
[5] Department of Electrical and Electronic Engineering, Imperial College of Science, Technology and Medicine, Exhibition Road, London SW7 2BT, United Kingdom

Received 5 October 2006

ABSTRACT: *Transmission properties of magnetoinductive waves propagating in two coupled one-dimensional metamaterial arrays are studied both experimentally and theoretically for the case when one of the arrays is shifted relative to the other one. Two different kinds of resonant metamaterial elements, split-pipe and spiral resonators, are investigated in the frequency bands centred at 46.2 and 586 MHz, respectively. It is shown that within a certain frequency range close to the resonant frequencies the transmission is strongly dependent on the shift. Theoretical calculations based on the impedance matrix show good agreement with the experimental results.* © 2007 Wiley Periodicals, Inc. Microwave Opt Technol Lett 49: 1054–1058, 2007; Published online in Wiley InterScience (www.interscience.wiley.com). DOI 10.1002/mop.22344

Key words: *metamaterials; magnetoinductive waves; magnetic coupling*

1. INTRODUCTION

The properties of metamaterials have been in the forefront of interest ever since Pendry's discovery [1] that, under certain circumstances, they are capable of producing not only negative refraction but perfect imaging as well. The conditions under which imaging can be realized have been widely investigated (see e.g. Refs. 2 and 3.) both theoretically and experimentally. A necessary consequence of this quest was the study of the properties of the actual elements [4–7] followed closely by further research on the interaction between the elements [8–11]. The most obvious and most effective interaction between the elements relies on magnetic coupling giving rise to magnetoinductive (MI) waves [8, 12]. This magnetic coupling between any two elements can be characterized by a mutual inductance whose value depends on the size and shape of the elements as well as on their relative orientation. In addition to the self-impedance, it plays a decisive role in the propagation properties of magnetoinductive waves, determines the direction of phase and group velocities, and gives the width of the frequency band in which the waves can propagate. Investigations carried out so far have been mainly concerned with arrays of identical elements in one- and two-dimensions [8, 12–14], although dispersion equations are also available for the three-dimensional case [12]. Coupling between arrays has also been considered with the purpose of producing waveguide components, filters, and delay lines [10, 11]. It has been shown for example that directional couplers for MI waveguides can be designed by specifying the mutual inductances in the coupling region.

The aim of the present article is to investigate both theoretically and experimentally the properties of two coupled arrays consisting of metamaterial elements when one of them is shifted mechanically relative to the other one. The theoretical analysis is based on the impedance matrix that relates the currents and applied voltages to each other. For a given excitation, the currents may then be obtained by inverting the impedance matrix.

In Section 2, we introduce the elements used and the experimental arrangement. The mathematical formulation and theoretical considerations are discussed in Section 3, results are shown in Section 4 and conclusions are drawn in Section 5.

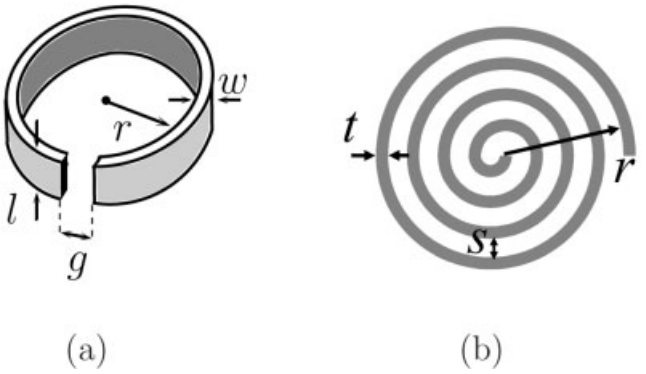

Figure 1 Schematic representation of (a) the split-pipe and (b) the spiral resonators

2. EXPERIMENT

Two different kinds of metamaterial elements were used in the experiments, capacitively loaded split-pipes and spirals, as shown in Figures 1(a) and 1(b). Their resonant frequencies and guiding properties were studied before [15–18]. The dimensions of the first type (the inner radius, width, height, and the width of the gap) are [Fig. 1(a)] $r = 10$ mm, $w = 1$ mm, $l = 5$ mm, and $g = 1$ mm. They are loaded by nominally identical capacitors of 330 pF. Their resonant frequencies and quality factors, measured with the aid of a network analyzer of the type HP8753C, were found as $f_0 = 42.6 \pm 0.2$ MHz and $Q = 105 \pm 5$, respectively.

The elements of the second type are four-turn spiral resonators produced on a Printed Circuit Board (type FR4) by selective etching as specified by a mask. Their radius, width of the spiral, and the separation between the turns are $r = 9$ mm, $t = 0.9$ mm, and $s = 1.35$ mm as may be seen in Figure 1(b). The resonance frequencies and quality factors of the spirals were measured as $f_0 = 0.586 \pm 0.004$ GHz and the quality factor as $Q = 49 \pm 4$.

2.1. Coupling Between the Elements

Next, we investigated magnetic coupling between two elements of the same kind both in the axial (centers of the elements lie on an axis perpendicular to their planes) and in the planar (the elements are in the same plane) configurations. A measure of magnetic coupling is the coupling coefficient

$$\kappa = 2M/L \tag{1}$$

where L is the self-inductance and M is the mutual inductance between the elements. The measurement is done by placing a transmitting coil near the centre of one element and then measuring the currents in both elements within a certain frequency range by moving a receiving coil consecutively to elements 1 and 2. The coupling coefficient may be then derived by determining the frequency variation of the currents.

The measurements for the split-pipes were performed at 401 discrete values of frequency in the range of 45–48 MHz. In the

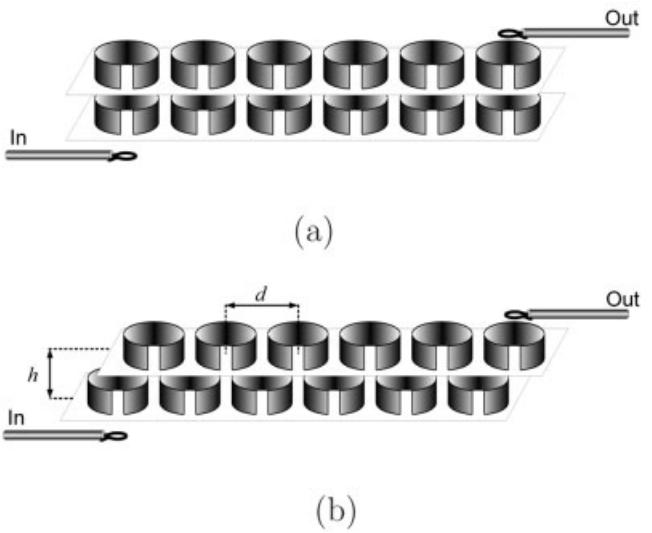

Figure 2 Schematic representation of the (a) unshifted and (b) half-a-period shifted coupled lines. The first element of the lower array is excited by a transmitting coil and the signal in the last element of the upper array is measured by a receiving coil

planar configuration, the distance between the centers of the elements was $d = 24$ mm yielding $\kappa_{\parallel} = -0.09$. In the axial configuration, the distance between the elements was $h = 5$ mm yielding $\kappa_{\perp} = 0.32$.

For the spirals, the measurements were performed at 1601 values of frequency between 0.3 and 0.9 GHz. The coupling coefficient in the planar arrangement for a distance of $d = 19$ mm was found as $\kappa_{\parallel} = -0.06$. In the axial configuration, the coupling coefficient was measured at distances $h = 5$ mm and $h = 10$ mm yielding $\kappa_{\perp} = 0.42$ and $\kappa_{\perp} = 0.14$, respectively.

2.2. Arrays

For each kind of elements, two planar lines consisting of 13 elements were produced. The split-pipes were placed on a piece of balsawood with a period of $d = 24$ mm between the centers of nearest neighbors. The arrays of spirals were produced on two pieces of PCB with a period of $d = 19$ mm.

2.3. Experimental Set-Up

Arrays of identical elements were placed exactly above each other so that the first elements of the upper and lower arrays were in an axial configuration as shown in Figure 2(a) for split-pipes. The first element of the lower array was excited by a transmitting coil and the signal in the last element of the upper array was measured by a receiving coil. The aim of the experiment is to measure the output to input ratio under the conditions when the upper array together with the receiving coil is mechanically shifted by different amounts, Δ, relative to the lower one. This is shown again for the split-pipes for a shift of half a period, $\Delta = d/2$, in Figure 2(b). The transmission as a function of frequency was then measured for a large number of shifts.

The measurements of the split-pipe arrays were performed for a spacing of $h = 10$ mm between the arrays. They were shifted over a total distance of $\Delta = 80$ mm relative to each other in steps of 2 mm, and the transmission was measured in the frequency range 34–58 MHz at 1601 discrete frequency points. The same experiments were conducted for the spiral arrays but for two different spacings, $h = 5$ mm and 10 mm, respectively. For both experiments, the upper array was shifted again over a total distance of 80 mm in steps of 2 mm. The measurements were performed at 1601 discrete values of frequency between 0.3 and 0.9 GHz.

3. THEORY

The theory of magnetoinductive waves is well known by now. Dispersion equations, derived on the assumption of nearest neighbor interactions [8, 12], were experimentally confirmed [13]. The present experimental results may be qualitatively explained by a theory based on a combination of nearest neighbor interactions and coupling between the arrays. We shall return to this in Section 4. In the present section, we shall be concerned with an alternative theory, which gives better quantitative agreement between theory and experiment. It is very general in the sense that it takes into account interaction between any two elements wherever they are. The relevant equation may be easily stated as

$$V = ZI \tag{2}$$

where $\mathbf{I}$ is a column-vector of the currents in the elements, $\mathbf{V}$ is a vector of the applied voltages, and $\mathbf{Z}$ is the matrix of self and mutual impedances. $Z_{m,n}$ relates the current in the n-th element to the voltage applied to the m-th element. Note that in our case, only the first element is excited so that all elements of the voltage vector with the exception of the first one are zero. The matrix has a dimension of $N \times N$, where N is the total number of elements, 26 in our case.

We have measured the resonant frequencies and quality factors of all the elements thus we know the diagonal elements of $\mathbf{Z}$ at all the frequencies considered. As for the mutual impedances, for each configuration only two values were measured. To determine the rest of the mutual impedances, we assumed that our elements may be modelled by loops with a radius equal to the radius of the actual elements (10 mm for the split-pipes and 9 mm for the spirals). It is then possible to calculate the mutual inductances between any two elements (see e.g. [19]). This is quite a simple calculation for the split-pipe arrays in which both the period and the total length of the structure are much smaller than the free-space wavelength at the operating frequencies. The retardation effects can then be neglected, and consequently the mutual impedance between the elements is purely imaginary i.e. only the mutual inductance, due to the magnetic coupling, is effective.

For the spiral arrays, the situation is different: the free space wavelength of about 500 mm is still much larger then the period ($d = 19$ mm); however, the total length of the arrays is above half wavelength when fully extended. Therefore, for more accurate calculations, retardation effects have to be taken into account. In the presence of retardation, the mutual inductance acquires an imaginary part and the decline of its real part with distance is less sharp. Since the calculated values of the mutual impedances agreed well with those measured (for nearest neighbors as described in the previous section), we could assume that all the mutual inductances calculated from our model were close to the actual ones. We obtained these way theoretical values for all the mutual inductances. Knowing both the voltage vector, $\mathbf{V}$, and the impedance matrix, $\mathbf{Z}$, we could determine the currents in each element for all frequencies and shifts by inverting numerically the relationship given by Eq. (2).

4. RESULTS

We shall now plot the experimentally obtained values of the transmission and compare them with theoretical results. For split-pipes, these are shown in Figures 3(a) and 3(b). The power transmitted from the first element of the lower array to the last

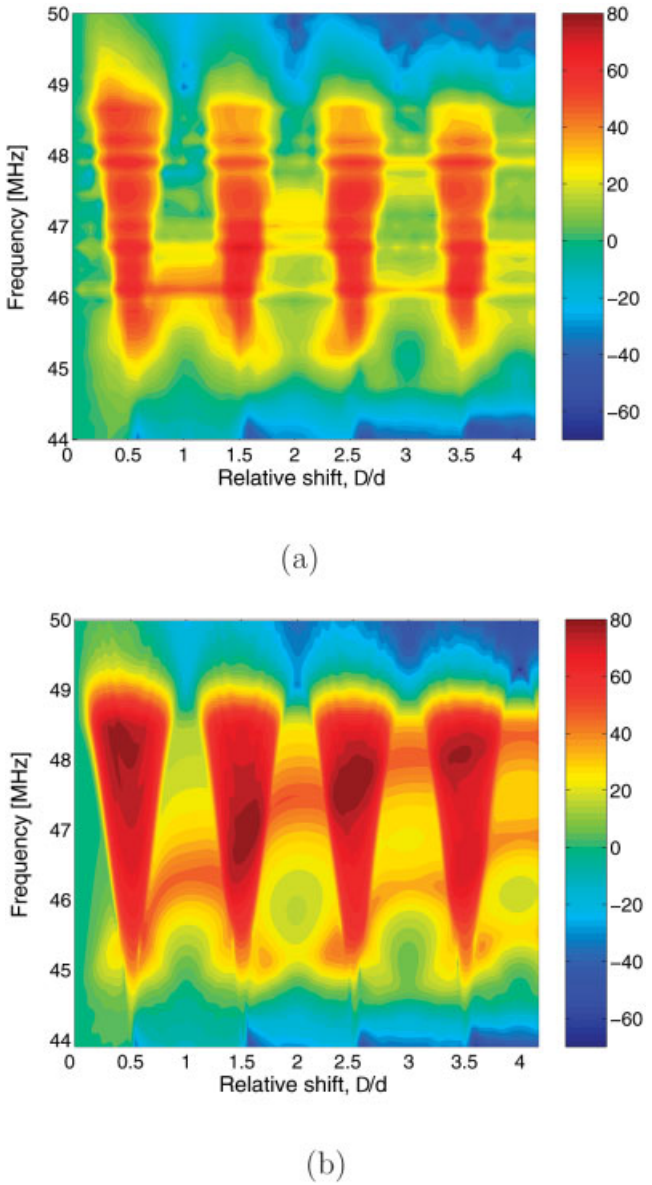

Figure 3 Contour plots of transmission between the split-pipe arrays ($h = 10$ mm) as a function of frequency and shift, (a) experiment, (b) theory. [Color figure can be viewed in the online issue, which is available at www.interscience.wiley.com]

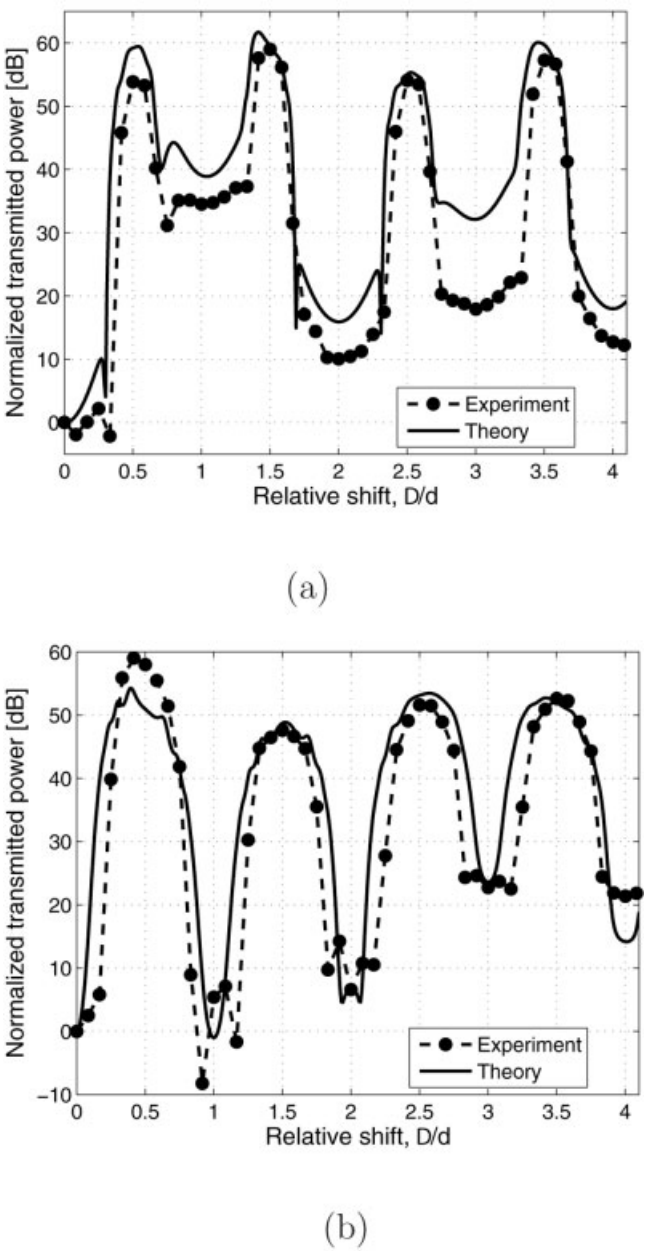

Figure 4 Transmitted power as a function of the shift between two split-pipe arrays, for different values of frequency, (a) $f = 46.2$ MHz, (b) $f = 48$ MHz. Dashed line with circles denotes experiment, solid line theory

element of the upper array is normalized to its value for zero shift and is shown as a contour plot. It may be seen that within a certain frequency range near the resonant frequency of the elements the transmission varies greatly with the shift. Transmission is minimum when the elements are above each other and maximum when the shift is half period, one and a half period, etc. The effect of the shift is quite radical: the difference between maximum and minimum transmission may be as much as 60 dB. The agreement between theory and experiment may be seen to be good in the whole frequency region.

To show the results in a more comparable and more quantitative form, we plotted the experimental (circles) and theoretical results (solid line) as a function of shift at two discrete frequencies in Figures 4(a) and 4(b). The vertical axis is in decibels. The curves are normalized to the value of transmission at zero shift. The two selected values of frequency are the resonant frequency, $f = 46.2$ MHz, and one above it at $f = 48$ MHz. The agreement may be seen to be remarkably good.

The transmission results for the arrays made up by spirals are presented in Figures 5 and 6 again in the form of contour plots for $h = 5$ mm and 10 mm, respectively. It is gratifying to note that although the operating frequencies for these measurements are ~10 times larger than those for split-pipes, the transmission of the spiral arrays (both for $h = 5$ mm and 10 mm) has a similar variation with shift: the regions of low and high transmission occur again for full period and half period shifts. The shape of high transmission regions is also similar: wider for the higher and narrower for the lower frequencies. The agreement appears to be better for $h = 5$ mm than for 10 mm. This can be explained by the fact that the latter configuration is more affected by retardation and

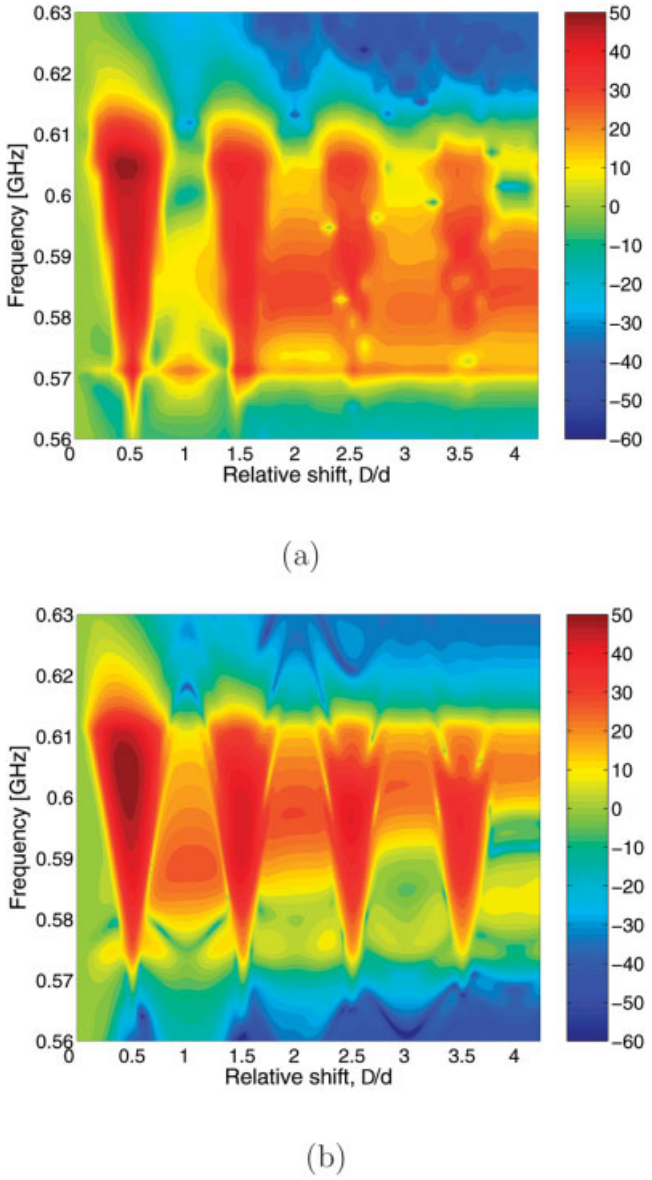

Figure 5 Contour plots of transmission between the spiral lines (h = 5 mm) as a function of frequency and shift, (a) experiment, (b) theory. [Color figure can be viewed in the online issue, which is available at www.interscience.wiley.com]

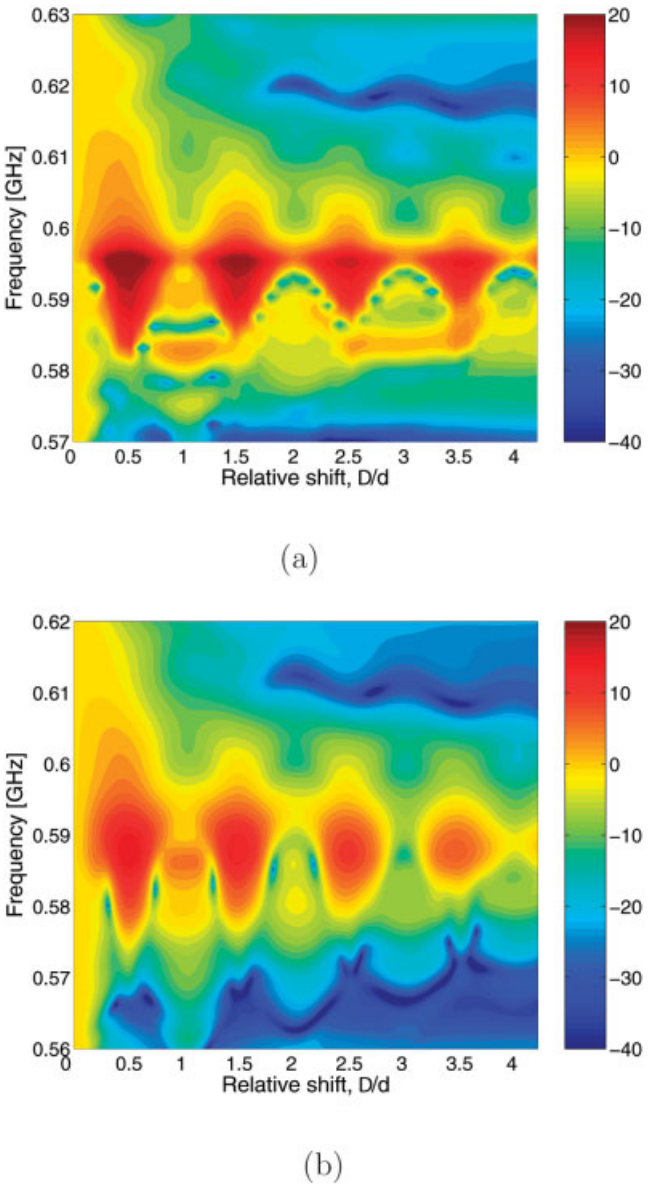

Figure 6 Contour plots of transmission between the spiral lines (h = 10 mm) as a function of frequency and shift, (a) experiment, (b) theory. [Color figure can be viewed in the online issue, which is available at www.interscience.wiley.com]

the model (replacing the actual elements by loops) is bound to be less accurate when retardation is present.

The measured high ratio between minima and maxima can be useful in the development of RF switches and signal flow controls with built-in frequency selectivity. Future work will further investigate these properties and develop new devices.

Next, we shall give a qualitative explanation of the transmission variation with the shift that is based on the theory of coupled magnetoinductive waveguides presented in Ref. 20. For this purpose, we choose the arrays made up by split-pipes. The dispersion curves of magnetoinductive waves for a lossless case are shown in Figure 7 for three different values of shift between the arrays, no shift (a), 0.35 d-shift (b), and half a period shift (c). The horizontal dashed lines indicate the resonant frequency, 46.2 MHz. As can be seen from Figure 7(a), when the arrays are not shifted relative to each other (or shifted by an integer number of periods) the resonant frequency lies in one of the stop-bands of the dispersion characteristics. Consequently, magnetoinductive waves do not propagate along the arrays and transmission is low. For the value of shift of 0.35d, the resonant frequency lies at the edge of the pass-band [see Fig. 7(b)], this is the amount of shift when the transmission between the lines should undergo an abrupt change. Indeed, as seen in Figure 4(a), in the vicinity of this point the transmission between the waveguides increases up to 50 dB. The resonant frequency is close to the middle of the pass-band for the shift of one half of the period [see Fig. 7(c)]. The losses are lower in the middle of the pass-band than at its edges and therefore the transmission is bound to be higher.

It also follows from this qualitative model that around 42 MHz transmission varies in an entirely different manner as may be seen from Figures 7(a)–(c): it is high for shifts corresponding to the whole period and low for half-period shifts. The effect is, however, less pronounced due to high losses at frequencies far from the resonant one.

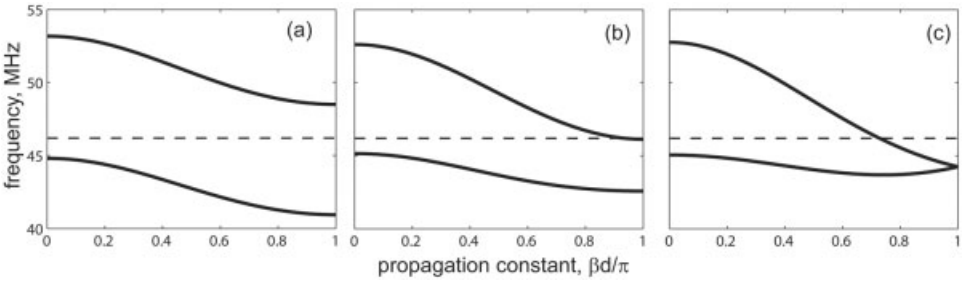

Figure 7 Dispersion of the magnetoinductive waves for arrays of split-pipes (a) nonshifted, (b) shifted by 0.35 of the period, and (c) shifted by half the period. No transmission at the resonant frequency (dashed lines) in case (a), abrupt increase of the transmission in case (b), and high transmission in case (c)

5. CONCLUSIONS

The efficacy of coupling between two one-dimensional arrays capable of propagating magnetoinductive waves has been investigated under the condition when one of the arrays is shifted relative to the other one. It has been shown that transmission of power from the input of the lower array to the output of the upper array depends crucially on the shift: there is minimum transmission for the unshifted case and maximum transmission for shifts of half a period. The maximum to minimum ratio has been as large as 60 dB making the effect potentially useful in devices. Good quantitative agreement has been found between experimental and theoretical results. A qualitative explanation based on path-bands and stop-bands has also been provided.

ACKNOWLEDGMENT

AR, MS, and CJS thank the financial support from the Royal Society Incoming Visitor Scheme and the Royal Society International Research Collaboration Grant. Financial support of the DFG (GK 695 and Emmy Noether-Programme) is gratefully acknowledged by OS and ES. MS is also supported by the Scheubeck-Jansen-Stiftung.

REFERENCES

1. J.B. Pendry, Negative refraction makes a perfect lens, Phys Rev Lett 85 (2000), 3966–3969.
2. E. Shamonina, V.A. Kalinin, K.H. Ringhofer, and L. Solymar, Imaging, compression and Poynting vector streamlines with negative permittivity materials, Electron Lett 37 (2001), 1243–1244.
3. M.J. Freire and R. Marques, A planar magnetoinductive lens for three-dimensional subwavelength imaging, Appl Phys Lett 86 (2005), 182505.
4. P. Gay-Balmaz and O.J.F. Martin, Electromagnetic resonances in individual and coupled split-ring resonators, J Appl Phys 92 (2002), 2929.
5. R. Marques, F. Medina, and R. Rafii-El-Idrissi, Role of bianisotropy in negative permeability and left-handed metamaterials, Phys Rev B 65 (2002), 144440.
6. M. Shamonin, E. Shamonina, V. Kalinin, and L. Solymar, Properties of a metamaterial element: Analytical solutions and numerical simulations for a singly split double ring, J Appl Phys 95 (2004), 3778–3784.
7. S. Maslovski, P. Ikonen, I. Kolmakov, S. Tretyakov, and M. Kaunisto, Artificial magnetic materials based on the new magnetic particle: Metasolenoid, Prog Electromagn Res 54 (2005), 61–81.
8. E. Shamonina, V.A. Kalinin, K.H. Ringhofer, and L. Solymar, Magneto-inductive waveguide, Electron Lett 38 (2002), 371–373.
9. C.R. Simovski, P.A. Belov, and S. He, Backward wave region and negative material parameters of a structure formed by lattices of wires and split-ring resonators, IEEE Trans Antennas Propag 51 (2003), 2582–2591.
10. M.J. Freire, R. Marques, F. Medina, M.A.G. Laso, and F. Martin, Planar magnetoinductive wave transducers: Theory and applications, Appl Phys Lett 85 (2004), 4439–4441.
11. I.S. Nefedov and S.A. Tretyakov, On potential applications of metamaterials for the design of broadband phase shifters, Microwave Opt Technol Lett 42 (2005), 98–101.
12. E. Shamonina, V.A. Kalinin, K.H. Ringhofer, and L. Solymar, Magnetoinductive waves in one, two, and three dimensions, J Appl Phys 92 (2002), 6552–6261.
13. M.C.K. Wiltshire, E. Shamonina, I.R. Young, and L. Solymar, Dispersion characteristics of magneto-inductive waves: Comparison between theory and experiment, Electron Lett 39 (2003), 215–217.
14. O. Zhuromskyy, E. Shamonina, and L. Solymar, 2D metamaterials with hexagonal structure: Spatial resonances and near field imaging, Opt Express 13 (2005), 9299–9309.
15. J.D. Baena, R. Marques, F. Medina, and J. Martel, Artificial magnetic metamaterial design by using spiral resonators, Phys Rev B 69 (2004), 014402.
16. A. Radkovskaya, M. Shamonin, C.J. Stevens, G. Faulkner, D.J. Edwards, E. Shamonina, and L. Solymar, Resonant frequencies of a combination of split rings: Experimental, analytical and numerical study. Microwave Opt Technol Lett 46 (2005), 473–476.
17. T. Hao, C.J. Stevens, and D.J. Edwards, Optimisation of metamaterials by Q factor. Electron Lett 41 (2005), 653–654.
18. G. Goussetis, A.P. Feresidis, S. Wang, Y. Guo, and J.C. Vardaxoglou, Uniplanar left-handed artificial metamaterials, J Opt A: Pure Appl Opt 7 (2005), 44–50.
19. L.D. Landau and E.M. Lifschitz, Electrodynamics of continuous media, Pergamon Press, Oxford, 1984.
20. O. Sydoruk, A. Radkovskaya, O. Zhuromskyy, E. Shamonina, M. Shamonin, C.J. Stevens, G. Faulkner, D.J. Edwards, and L. Solymar, Tailoring the near-field guiding properties of magnetic metamaterials with two resonant elements per unit cell, Phys Rev B 73 (2006), 224406.

ANALYSIS OF THE BAND-STOP TECHNIQUES FOR ULTRAWIDEBAND ANTENNA

Seokjin Hong, Jaewoong Shin, Hoon Park, and Jaehoon Choi
Department of Electrical and Computer Engineering, Hanyang University, 17 Haengdang-dong, Seongdong-Gu, Seoul 133–791, Korea

Received 14 September 2006

ABSTRACT: *Two band-stop techniques for UWB antenna design are suggested in this article. The proposed antennas have wide bandwidth enough to cover UWB services along with the band-stop characteristic for 5 GHz WLAN band. By inserting an U-shaped slot or attaching an*